Anal. Chem. **2001,** *73,* 5743−5751

Spectroscopic Investigations of Poly(Propyleneimine)Dendrimers Using the Solvatochromic Probe Phenol Blue and Comparisons to Poly(Amidoamine) Dendrimers

Dana L. Richter-Egger,† Aaron Tesfai, and Sheryl A. Tucker*

Department of Chemistry, University of Missouri−Columbia, Columbia, Missouri 65211-7600

The physical and chemical properties of PPI dendrimers' interior were investigated using the fluorescent, solvatochromic probe phenol blue. In aqueous solutions of each generation studied, two discrete dye populations were clearly observed. PPI dendrimers were shown to form a tight, nonpolar association with the vast majority of available dye, within the dendrimer interior, near the core. In the steady-state fluorescence emission spectra, a microenvironment of decreasing polarity in increasingly larger-generation PPI dendrimers (up to G3) was seen for the associated probe. Each of the remaining larger-generation dendrimers provided a microenvironment of essentially equal polarity. Fluorescence anisotropy values for phenol blue in the PPI dendrimers demonstrated the dye's sensitivity to the changing molecular volumes of the dendrimer generations. Model compounds that mimicked PPI's surface groups and branching moieties were used to better define the associated dye's location. The mimics further confirmed that phenol blue was associated inside the dendrimer, where it did not interact with the dendrimer surface groups. The comparison of amine-terminated PPI and PAMAM dendrimers clearly demonstrated the effects of their structural differences and the ability of phenol blue to have sensed those differences, including the initiator core length, branching unit length, and branching unit chemical composition.

Dendrimers are a unique, highly diverse class of polymers that, unlike traditional polymers, have well-defined macromolecular architecture. They are constructed by the iterative addition of branching unit layers, called generations (G), to a polyfunctional core atom or molecule. This is described pictorially for poly(propyleneimine), PPI, dendrimers in Figure 1. Dendrimers are described as unimolecular micelles[1−4] because of their similar structural features. However, micelles form only at concentrations above the critical micelle concentration, vary significantly in size and shape, and are dynamic systems in which free surfactant monomers continuously migrate into and out of the micelle. Dendrimers do not share these properties. Instead, they are monodisperse,[5] covalently bound molecules at all concentrations, stable over a large pH range,[6] and easily functionalized[7,8] to tailor their solubility and stability for use in many organic solvents. Therefore, the substitution of dendrimers into current micellar applications may be particularly useful. Suggested dendrimer applications are as diverse as their structures. For example, they have been used as gene transfer agents,[9−12] a promising AIDS

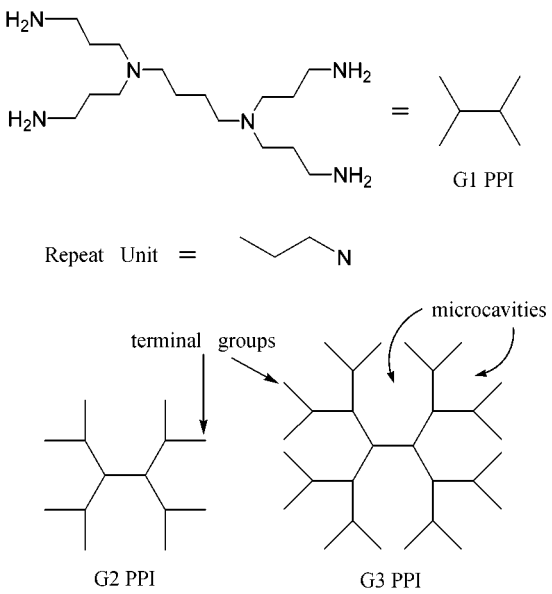

Figure 1. Architecture of a PPI dendrimer (modeled after Chart 1 in ref 37).

* To whom correspondence should be addressed. E-mail: TuckerS@missouri.edu.

† Current address: Department of Chemistry, University of Nebraska at Omaha, Omaha, NE 68182-0109.

(1) Piotti, M. E.; Rivera, F., Jr.; Bond, R.; Hawker, C. J.; Fréchet, J. M. J. *J. Am. Chem. Soc.* **1999**, *121*, 9471−9472.

(2) Hawker, C. J.; Wooley, K. L.; Fréchet, J. M. *J. Chem. Soc., Perkin Trans. 1* **1993**, *1*, 1287−1297.

(3) Tomalia, D. A.; Berry, V.; Hall, M.; Hedstrand, D. M. *Macromolecules* **1987**, *20*, 1164−1167.

(4) Newkome, G. R.; Moorefield, C. N.; Baker, G. R.; Saunders, M. J.; Grossman, S. H. *Angew. Chem., Int. Ed. Engl.* **1991**, *30*, 1178−1180.

(5) Li, J.; Piehler, L. T.; Qin, D.; Baker, J. R., Jr.; Tomalia, D. A.; Meier, D. J. *Langmuir* **2000**, *16*, 5613−5616.

(6) Tomalia, D. A.; Naylor, A. M.; Goddard, W. A., III. *Angew. Chem., Int. Ed. Engl.* **1990**, *29*, 138−175.

(7) Leon, J. W.; Kawa, M.; Fréchet, J. M. *J. Am. Chem. Soc.* **1996**, *118*, 8847−8859.

(8) Palmer, C. P. *J. Chromatogr. A* **1997**, *780*, 75−92.

(9) Haensler, J.; Szoka, F. C., Jr. *Bioconjugate Chem.* **1993**, *4*, 372−379.

10.1021/ac0155355 CCC: $20.00
Published on Web 10/30/2001

vaccine,[13] catalysts,[14−17] radiotheraputic agents,[18] and substitutes for micelles in micellar electrokinetic chromatography.[8,19−23]

Two families of dendrimers, PPI and poly(amidoamine) (PAMAM), are commercially available in many different sizes/generations, and the PAMAM dendrimers have received considerable attention. Spectroscopic methods have been effectively used to study both the surfaces[24−37] and the interior regions[37−40] of PAMAM dendrimers. However, significantly less information is published about the PPI dendrimers. In fact, to our knowledge, very little spectroscopic evidence has been published concerning the PPI dendrimer interior. An improved understanding of the chemical and physical properties of the interior regions of PPI dendrimers is vital to their successful use in future applications.

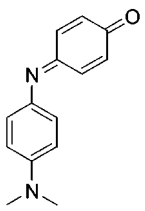

Figure 2. Chemical structure of phenol blue.

Previous studies of PPI dendrimers include surface characterization through periphery modification,[41−44] density profile characterization,[45−51] and host−guest characterization with anionic solute molecules.[52,53] One recent study of PPI dendrimers with the well-known fluorescent, solvent polarity probe pyrene, reported association of pyrene in the dendrimer interior.[54] Although the association provided information on the interior polarity, protection from aqueous sodium iodide and binding constants, the study only included the two large generations, G4 and G5. Our previous studies[39,40] demonstrated that important generational relationships can be revealed by examining a number of dendrimer generations.

The purpose of this work is to advance the knowledge of the novel microenvironments contained within the PPI dendrimers, specifically their accessibility, polarity, relative size, and generational dependence, for the five available generations. Our approach is to use the solvatochromic probe phenol blue (Figure 2) in the same manner that we effectively probed the interior regions of amine-terminated PAMAM (PAMAM-AT) dendrimers in our previous study.[39] Spectrofluorometric probe techniques provide realistic views of macromolecular media in fluid solution.[55−57] They are especially powerful when used in combination and enable one to develop a more comprehensive and accurate picture.[58,59] Important advantages of fluorescence spectroscopy include minimal sample perturbation, high sensitivity, and subnanomolar

(10) Tang, M.; Redemann, C. T.; Szoka, F. C., Jr. *Bioconjugate Chem.* **1996**, *7*, 703−714.
(11) Ukowska-Latallo, J. F.; Bielinska, A. U.; Johnson, J.; Spindler, R.; Tomalia, D. A.; Baker, J. R. J. *Proc. Natl. Acad. Sci. U.S.A.* **1996**, *1993*, 4897−4902.
(12) Bielinska, A.; Kukowska-Latallo, J.; Johnson, J.; Tomalia, D. A.; Baker, J. R. J. *Nucleic Acids Res.* **1996**, *24*, 2176−2182.
(13) Defoort, J. P.; Nardelli, B.; Huang, W.; Ho, D. D.; Tam, J. P. *Proc. Natl. Acad. Sci. U.S.A.* **1992**, *89*, 3879−3883.
(14) Issberner, J.; Böhme, M.; Grimme, S.; Nieger, M.; Paulus, W.; Vögtle, F. *Tetrahedron: Asymmetry* **1996**, *7*, 2223−2232.
(15) Suh, J.; Hah, S. S.; Lee, S. H. *Bioorg. Chem.* **1997**, *25*, 63−75.
(16) Chow, H.-F.; Mak, C. C. *J. Org. Chem.* **1997**, *62*, 5116−5127.
(17) Bardaji, M.; Caminade, A.-M.; Majoral, J.-P.; Chaudret, B. *Organometallics* **1997**, *16*, 3489−3497.
(18) Martin, V. V.; Ralston, W. H.; Hynes, M. R.; Keana, J. F. W. *Bioconjugate Chem.* **1995**, *6*, 616−623.
(19) Gao, H.; Carlson, J.; Stalcup, A. M.; Heineman, W. R. *J. Chromatogr. Sci.* **1998**, *36*, 146−154.
(20) Tanaka, N.; Tanigawa, T.; Hosoya, K.; Kimata, K.; Araki, T.; Terabe, S. *Chem. Lett.* **1992**, 959−962.
(21) Kuzdzal, S. A.; Monnig, C. A.; Newkome, G. R.; Moorefield, C. N. *J. Chem. Soc., Chem. Commun.* **1994**, *18*, 2139−2140.
(22) Kuzdzal, S. A.; Monnig, C. A.; Newkome, G. R.; Moorefield, C. N. *J. Am. Chem. Soc.* **1997**, *119*, 2255−2261.
(23) Muijselaar, P. G. H. M.; Claessens, H. A.; Cramers, C. A.; Jansen, J. F. G. A.; Meijer, E. W.; de Brabander-van den Berg, E. M. M.; van der Wal, S. *J. High Resolut. Chromatogr.* **1995**, *18*, 121−123.
(24) Turro, N. J. *Pure Appl. Chem.* **1995**, *67*, 199−208.
(25) Caminati, G.; Turro, N. J.; Tomalia, D. A. *J. Am. Chem. Soc.* **1990**, *112*, 8515−8522.
(26) ben-Avraham, D.; Schulman, L. S.; Bossmann, S. H.; Turro, C.; Turro, N. J. *J. Phys. Chem. B* **1998**, *102*, 5088−5093.
(27) Gopidas, K.; Leheny, A. R.; Caminati, G.; Turro, N. J.; Tomalia, D. A. *J. Am. Chem. Soc.* **1991**, *113*, 7335−7342.
(28) Ottaviani, M. F.; Bossmann, S.; Turro, N. J.; Tomalia, D. A. *J. Am. Chem. Soc.* **1994**, *116*, 661−671.
(29) Jockusch, S.; Ramirez, J.; Sanghvi, K.; Nociti, R.; Turro, N. J.; Tomalia, D. A. *Macromolecules* **1999**, *32*, 4419−4423.
(30) Moreno-Bondi, M. C.; Orellana, G.; Turro, N. J. *Macromolecules* **1990**, *23*, 910−912.
(31) Wade, D. A.; Torres, P. A.; Tucker, S. A. *Anal. Chim. Acta* **1999**, *397*, 17−31.
(32) Ottaviani, M. F.; Turro, C.; Turro, N. J.; Bossmann, S. H.; Tomalia, D. A. *J. Phys. Chem.* **1996**, *100*, 13667−13674.
(33) Turro, C.; Niu, S.; Bossmann, S. H.; Tomalia, D. A.; Turro, N. J. *J. Phys. Chem.* **1995**, *99*, 5512−5517.
(34) Jockusch, S.; Turro, N. J.; Tomalia, D. A. *Macromolecules* **1995**, *28*, 7416−7418.
(35) Ottaviani, M. F.; Turro, N. J.; Jockusch, S.; Tomalia, D. A. *J. Phys. Chem.* **1996**, *100*, 13675−13686.
(36) Drummond, C. J.; Grieser, F.; Healy, T. W. *J. Chem. Soc., Faraday Discuss.* **1986**, *81*, 95−106.
(37) Pistolis, G.; Malliaris, A.; Paleos, C. M.; Tsiourvas, D. *Langmuir* **1997**, *13*, 5870−5875.
(38) Larson, C. L.; Tucker, S. A. *Appl. Spectrosc.* **2001**, *55*, 679−683.
(39) Richter-Egger, D. L.; Landry, J. C.; Tesfai, A.; Tucker, S. A. *J. Phys. Chem. A* **2001**, *105*, 6826−6833.
(40) Richter-Egger, D. L.; Li, H.; Tucker, S. A. *Appl. Spectrosc.* **2000**, *54*, 1151−1156.
(41) Baker, L. A.; Crooks, R. M. *Macromolecules* **2000**, *33*, 9034−9039.
(42) Yeow, E. K. L.; Ghiggino, K. P.; Reek, J. N. H.; Crossley, M. J.; Bosman, A. W.; Schenning, A. P. H. J.; Meijer, E. W. *J. Phys. Chem. B* **2000**, *104*, 2596−2606.
(43) Balzani, V.; Ceroni, P.; Gestermann, S.; Kauffmann, C.; Gorka, M.; Vögtle, F. *Chem. Commun.* **2000**, 853−854.
(44) Vögtle, F.; Gestermann, S.; Kauffmann, C.; Ceroni, P.; Vicinelli, V.; Cola, L. D.; Balzani, V. *J. Am. Chem. Soc.* **1999**, *121*, 12161−12166.
(45) Murat, M.; Grest, G. S. *Macromolecules* **1996**, *29*, 1278−1285.
(46) Rietveld, I. B.; Bedeaux, D.; Smit, J. A. M. *J. Colloid Interface Sci.* **2000**, *232*, 317−325.
(47) Scherrenberg, R.; Coussens, B.; van Vliet, P.; Edouard, G.; Brackman, J.; de Brabander, E. *Macromolecules* **1998**, *31*, 456−461.
(48) Boris, D.; Rubinstein, M. *Macromolecules* **1996**, *29*, 7251−7260.
(49) Welch, P.; Muthukumar, M. *Macromolecules* **1998**, *31*, 5892−5897.
(50) Rietveld, I. B.; Bedeaux, D. *Macromolecules* **2000**, *33*, 7912−7917.
(51) Put, E. J. H.; Clays, K.; Persoons, A.; Biemans, H. A. M.; Luijkx, C. P. M.; Meijer, E. W. *Chem. Phys. Lett.* **1996**, *260*, 136−141.
(52) Miklis, P.; Çagin, T.; Goddard, W. A. I. *J. Am. Chem. Soc.* **1997**, *119*, 7458−7462.
(53) Baars, M. W. P. L.; Froehling, P. E.; Meijer, E. W. *Chem. Commun.* **1997**, 1959−1960.
(54) Pistolis, G.; Malliaris, A.; Tsiourvas, D.; Paleos, C. M. *Chem. Eur. J.* **1999**, *5*, 1440−1444.
(55) Warner, I. M.; McGown, L. B. *Anal. Chem.* **1992**, *64*, 343R−352R.
(56) Agbaria, R. A.; Roberts, E.; Warner, I. M. *J. Phys. Chem.* **1995**, *99*, 9, 10056−10060.
(57) Villegas, M. M.; Neal, S. L. *J. Phys. Chem. A* **1997**, *101*, 6890−6896.
(58) Li, G.; McGown, L. B. *J. Phys. Chem.* **1994**, *98*, 13711−13719.
(59) Warner, I. M.; Patonay, G.; Thomas, M. P. *Anal. Chem.* **1985**, *57*, 463A−483A.

detection limits.[60,61] The combination of solvatochromic absorption and fluorescence behavior and relatively small size make phenol blue a good choice for this study. In contrast to previous fluorescent probe studies,[25,37] the fluorescence emission of phenol blue is not quenched by the PPI dendrimer's tertiary amine groups. In addition, this study provides a more complete view of the interior region and generational dependencies through the use of additional spectroscopic techniques compared to previous studies of PPI dendrimers. A discussion is also included that compares these findings to those for PAMAM-AT dendrimers.

The physical[62−64] and spectroscopic absorption properties[65−68] of phenol blue have been well characterized, and the dye is believed to exist solely as the neutral quinoneimine[62] in both protic and aprotic solvents of varying polarities. The dye's solvatochromic absorption band shifts to shorter wavelengths as the solvent polarity decreases and has a λ_{max} range from 660 nm in trifluoroethanol to 550 nm in *n*-heptane.[65] To our knowledge, with the exception of our previous study[39] and the brief mention of its surface association with [8^2•3]micellanotes,[4] phenol blue has not been used to study organized media, but its structural analogue nile red, which is also a solvatochromic probe, has been used extensively to study proteins, lipids, enzymes, and PAMAM dendrimers with modified cores.[69−73] Mimics of PPI's surface and branching moieties are also examined to help determine the associated dye location.

EXPERIMENTAL SECTION

Materials. Amine-terminated PPI dendrimers with tetrafunctional diaminobutane cores were obtained as 25 wt % aqueous solutions (G1 and G2) or as neat liquids (G3−G5) (Aldrich) and stored at 5 °C. Other materials that were obtained were phenol blue, propylamine, and triethylamine from Aldrich and HPLC-grade water from Fisher. All chemicals were used as received.

Sample Preparation. Samples were prepared by quantitatively transferring known aliquots of the phenol blue stock solution into volumetric flasks, where the solvent was stripped off under ultrahigh-purity nitrogen. Appropriate volumes of aqueous PPI dendrimer stock solutions were quantitatively transferred to the flasks. The samples were diluted to volume with HPLC-grade water unless otherwise noted: [phenol blue] = 1×10^{-6} M and [dendrimer] = 1×10^{-4} M. These samples were stirred for ∼24 h to facilitate dye and dendrimer solubilization, followed by an additional ∼24 h equilibration in the dark at room temperature.

Methods. *UV/Vis Absorption Measurements.* Absorption spectra were collected in 1-cm^2 Suprasil quartz cuvettes on a Hitachi U-3000 (Hitachi Instruments, Danbury, CT) double-beam spectrophotometer at a scan rate of 120 nm/min, slit width of 1 nm, and thermostated cell temperature of 25 °C. Spectra were blank-corrected for the possible absorption of solvent and the aqueous dendrimers, although no background signal due to the dendrimers was apparent in the wavelength region of interest.

The software program PeakFit 4.0 for Windows (SPSS Inc. Chicago, IL) was used to deconvolute the overlapping bands present in the absorption spectra. A Gaussian−Lorentzian cross-product function afforded the best fit using automated peak deconvolution. (The aqueous band was forced to remain at 654 nm and have a value of 0.5 for the a_3 parameter, which controls the degree of Gaussian vs Lorentzian character.) For all other bands, the amplitude, center, width, and shape were allowed to vary according to the best fit. No baseline corrections were made during deconvolution.

Steady-State Fluorescence Measurements. The fluorescence emission spectra and steady-state anisotropy data were collected in 1-cm^2 Suprasil quartz cuvettes on an SLM 48000 DSCF/MHF spectrofluorometer (Jobin Yvon, Edison, NJ) at a thermostated temperature of 25 °C. The excitation source was an Ion Laser Technology (Salt Lake City, UT) RPC-50-220 argon ion laser operated at 514 nm and 30 mW.

For fluorescence emission spectra, the emission monochromator slit widths (entrance and exit) were set at 16 and 4 nm, respectively. The emission scan interval was 1 nm, and measurements were recorded from an internal average of three signal samplings/emission wavelength. The fluorescence emission was passed through a Glan Thompson polarizer set at 0° (vertical) to correct for the Woods anomaly.[74] Spectra were also absorption- and solvent-blank-corrected.

Steady-state anisotropy measurements were collected in "L" format[75] using Glan Thompson polarizers, a 550-nm long-pass filter (KV550 Schott Glass Technologies, Duryea, PA), and a 600-nm short-pass filter (03 SWP 610 Melles Griot, Irvine, CA). The means and standard deviations were calculated from five sample replicates, each containing an internal average of five signal samplings at each of the four polarizer orientations (0−0°, 0−90°, 90−0°, and 90−90°).

Fluorescence Lifetime Measurements. Fluorescence lifetimes were collected in the frequency domain,[76,77] on the same SLM 48000 DSCF/MHF spectrofluorometer, which also has multiharmonic, Fourier transform phase-modulation capabilities. The excitation source was a Coherent (Santa Clara, CA) Innova 307C argon ion laser operating at 514 nm and 500 mW. In MHF mode, however, only a small fraction of the excitation power is actually used to interrogate the sample. A base frequency of 4.0 MHz and a cross-correlation frequency of 7.000 Hz were used in all dynamic measurements. Ten pairs of sample/reference measurements were collected in triplicate for each sample, and each measure-

(60) McGown, L. B.; Hemmingsen, S. L.; Shaver, J. M.; Geng, L. *Appl. Spectrosc.* **1995**, *49*, 60−66.
(61) Geng, L.; McGown, L. B. *Anal. Chem.* **1992**, *64*, 68−74.
(62) Morley, J. O.; Fitton, A. L. *J. Phys. Chem. A* **1999**, *103*, 11442−11450.
(63) Figueras, J. *J. Am. Chem. Soc.* **1971**, *93*, 3255−3263.
(64) Kolling, O. W. *J. Phys. Chem.* **1991**, *95*, 3950−3954.
(65) Kolling, O. W. *Anal. Chem.* **1981**, *53*, 54−56.
(66) Kolling, O. W.; Goodnight, J. L. *Anal. Chem.* **1973**, *45*, 160−164.
(67) Kolling, O. W.; Goodnight, J. L. *Anal. Chem.* **1974**, *46*, 482−485.
(68) Kolling, O. W. *Anal. Chem.* **1978**, *50*, 212−215.
(69) Ruvinov, S. B.; Yang, X.-J.; Parris, K. D.; Banik, U.; Ahmed, S. A.; Miles, E. W.; Sackett, D. L. *J. Biol. Chem.* **1995**, *270*, 6357−6369.
(70) Sackett, D. L.; Wolff, J. *Anal. Biochem.* **1987**, *167*, 228−234.
(71) Sackett, D. L.; Knutson, J. R.; Wolff, J. *J. Bio. Chem.* **1990**, *265*, 14899−14906.
(72) Daban, J.-R.; Bartolomé, S.; Samsó, M. *Anal. Biochem.* **1991**, *199*, 169−174.
(73) Watkins, D. M.; Sayed-Sweet, Y.; Klimash, J. W.; Turro, N. J.; Tomalia, D. A. *Langmuir* **1997**, *13*, 3136−3141.
(74) Kessel, D. *Photochem. Photobiol.* **1991**, *54*, 481−483.
(75) Lakowicz, J. R. *Principles of Fluorescence Spectroscopy*; Plenum Press: New York, 1983.
(76) Spencer, R. D. Ph.D. Dissertation, University of Illinois, Urbana-Champaign, IL, 1970.
(77) Mitchell, G.; Swift, K. *Time-Resolved Laser Spectrosc. Biochem. II* **1990**; 270−274.

ment contained 100 internal averages. An aqueous scatter solution of kaolin (Sigma) was used as the lifetime reference. The same 550 long-pass/600 short-pass filter combination used for anisotropy measurements was also used for the lifetime measurements.

The lifetimes and fractional intensities were obtained from the phase and modulation data using the maximum entropy method (MEM).[78−80] Advantages of using MEM compared to traditional nonlinear least squares (NLLS) are documented and include the fact that MEM is self-modeling, does not require selection of an a priori model, and returns more consistent lifetime distributions.[57,60,79−82] The three replicate phase and modulation data sets collected for each sample were analyzed both individually and as a combined file. The lifetime window consisted of 500 discrete, equally spaced cells from 0.01 to 10 ns.

RESULTS

Solvatochromic Behavior of Phenol Blue. Because of variations in instrumental and experimental conditions from laboratory to laboratory,[83−85] in-house absorption and fluorescence "solvent polarity rulers" for phenol blue were generated and reported in our previous work.[39] Experimentally obtained absorption λ_{max} values were in good agreement with the literature[65] and ranged from 541 nm in *n*-heptane to 652 nm in water.[39] The previously unreported fluorescence emission λ_{max} varied from 602 nm in acetone to 620 nm in methanol.[39] These solvent polarity experiments also indicated that the dye's fluorescence quantum yield markedly decreases, and eventually the signal becomes virtually absent at the two solvent polarity extremes, such as *n*-heptane and water. We continue to investigate this observation. It is also important to note that although the amine-terminated PPI dendrimers are slightly basic (measured pH = 8−10), the observed λ_{max} shifts are not due to a pH response by phenol blue. The dye showed only a very small blue shift (5 nm) in its solvatochromic absorption band within this pH range.

UV/Vis Absorption Spectroscopy. Representative absorption spectra of phenol blue in water and aqueous PPI dendrimers are shown in Figure 3. All spectra, with the exception of the water spectrum, clearly show varying contributions from the same two absorption bands. The band at approximately 554 nm is due to a rather nonpolar microenvironment, and the band at 654 nm is indicative of a much more polar microenvironment, believed to be predominantly aqueous. The absorption spectrum of phenol blue in G1 PPI is distinctly different from the other four generations. It has two absorption bands that are nearly equal in intensity and are each somewhat blue-shifted compared to the other generations. The remaining four larger generations are all very similar; however, for successively larger generations of PPI, the band indicative of a relatively nonpolar microenvironment increases slightly in intensity at the expense of the band due to the predominantly aqueous microenvironment. In fact, G4 and G5 PPI have almost no significant contribution from the 654-nm band that represents the aqueous microenvironment. It should be noted that occasionally, a low-intensity, broad-absorption band around 460 nm (outside the solvatochromic region) was observed for some G4 and G5 phenol blue samples.

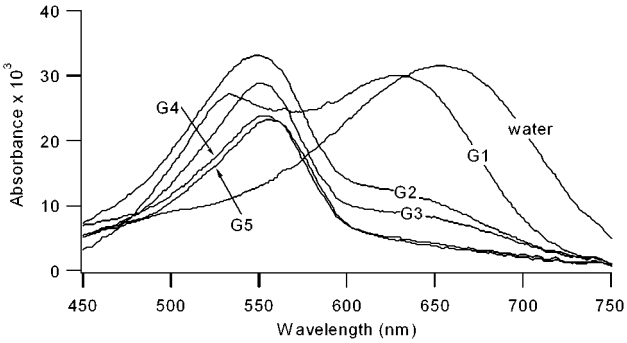

Figure 3. Representative absorption spectra of phenol blue [1 × 10^{-6} M] in aqueous PPI dendrimers [1 × 10^{-4} M]. Experimental conditions: T = 25 °C.

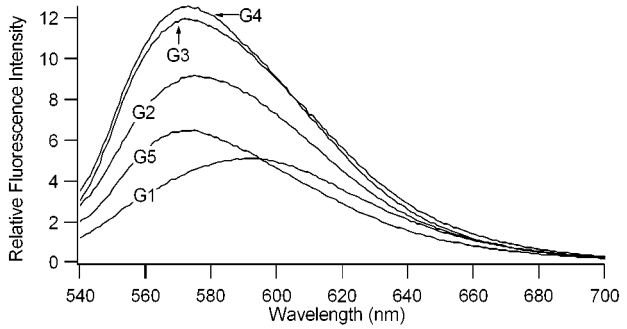

Figure 4. Representative steady-state fluorescence emission spectra of phenol blue [1 × 10^{-6} M] in PPI dendrimers [1 × 10^{-4} M], absorption- and blank-corrected. Experimental conditions: λ_{ex} = 514 nm and T = 25 °C.

Deconvolution of the G1 PPI absorption spectrum revealed two absorption bands (λ_{max} 531 and 632 nm) that fit the original spectrum without any major deviations. Deconvolution of all the other generations consistently revealed one band at λ_{max} 654 nm and another at λ_{max} 546 ± 2 nm. The λ_{max} of the 546-nm band was blue-shifted 5−8 nm, as compared to the original spectra, because of the effect of fitting this asymmetric band with a symmetric model.

Steady-State Fluorescence Emission Spectroscopy. Representative fluorescence spectra, corrected for the solvent and differential absorption at the excitation wavelength, are shown in Figure 4. Phenol blue in the presence of aqueous PPI dendrimers has a single, broad solvatochromic fluorescence emission band. There is a gradual blue shift of this band from G1 to G3, indicating decreased microenvironmental polarity. The remaining two generations have identical λ_{max} values as G3. The relative fluorescence intensity also significantly increases up through G3; however, the fluorescence intensity of G4 is only slightly greater than G3, and that of G5 is markedly decreased. No fluorescence spectrum for phenol blue in water could be obtained under steady-state conditions, which employ a monochromator.

Anisotropy values of the phenol blue−dendrimer solutions are shown in Table 1. These values systematically increase in a fairly linear fashion (r^2 = 0.87) from G1 to G5. The difference between

(78) Brochon, J. C.; Livesey, A. K.; Pouget, J.; Valeur, B. *Chem. Phys. Lett.* **1990**, *174*, 517−522.
(79) Shaver, J. M.; McGown, L. B. *Anal. Chem.* **1996**, *68*, 611−620.
(80) Shaver, J. M.; McGown, L. B. *Anal. Chem.* **1996**, *68*, 9−17.
(81) Neal, S. L. *J. Phys. Chem. A* **1997**, *101*, 6883−6889.
(82) Neal, S. L. *Anal. Chem.* **1997**, *69*, 5109−5120.
(83) Tucker, S. A. Ph.D. Dissertation, University of North Texas, Denton, TX, 1994.
(84) Street, K. W., Jr.; Acree, W. E., Jr. *Analyst* **1986**, *111*, 1197−1201.
(85) Meyerhoffer, S. M.; McGown, L. B. *Anal. Chem.* **1991**, *63*, 2082−2086.

Table 1. Representative Values for PAMAM and PPI Dendrimers[a]

	absorption λ_{max} (nm)		fluorescence λ_{max} (nm)		fluorescence anisotropy[b]		K_D/1000	
no. of SG	PAMAM	PPI	PAMAM	PPI	PAMAM	PPI	PAMAM[c]	PPI
4	642	629	598	588	0.096	0.061	2.7	8.4
8	640	549	582	578	0.151	0.159	4.3	87
16	562	551	578	573	0.183	0.160	14	170
32	558	554	574	573	0.214	0.235	28	780
64	557	557	572	573	0.260	0.275	80	4400

[a] Phenol blue [1×10^{-6} M] in aqueous PAMAM or PPI dendrimers [1×10^{-4} M]. Experimental conditions: absorption and fluorescence measurements taken at $T = 25$ °C and fluorescence $\lambda_{ex} = 514$ nm. [b] Standard deviations range from 0.002 to 0.007 for all generations of PPI and 0.004−0.01 for all generations of PAMAM. [c] The phenol blue−PAMAM molar absorptivities were determined using G5 PAMAM in the same manner as phenol blue in G4 PPI. The following molar absorptivities were recovered: $\epsilon_{free:654} = 15\,710$, $\epsilon_{free:556} = 6810$, $\epsilon_{complex:654} = 3400$, and $\epsilon_{complex:556} = 13\,530$.

Table 2. Representative Fluorescence Lifetimes and Fractional Intensity Contributions Recovered from MEM Analysis

medium	τ_1 (α_1)[a]	τ_2 (α_2)	τ_3 (α_3)
water	0.06 (0.64)		2.48 (0.36)
G1	0.19 (0.39)	0.87 (0.54)	3.06 (0.07)
G2	0.22 (0.42)	1.03 (0.52)	2.96 (0.06)
G3	0.24 (0.38)	1.22 (0.52)	3.17 (0.10)
G4	0.19 (0.38)	0.97 (0.50)	2.81 (0.11)
G5	0.20 (0.59)	1.09 (0.32)	3.45 (0.08)

[a] Results are averages of three replicate measurements of the same sample. Experimental conditions: $\lambda_{ex} = 514$ nm, $\lambda_{em} = 550-600$ nm, kaolin lifetime reference $\tau = 0$ ns, and $T = 25$ °C.

the values for G2 and G3 is considerably smaller than any other two consecutive generations.

Fluorescence Lifetimes. Table 2 shows representative fluorescence lifetimes (τ) and fractional intensity contributions (α) for phenol blue in PPI dendrimers recovered by MEM analysis.[78] A representative MEM lifetime distribution is also shown in Figure 5. Three lifetime components were recovered for most samples studied. The lifetimes and the associated fractional intensities remain relatively constant across dendrimer generations. The shortest lifetime component, τ_1, is observed in both samples and blanks. Shaver and McGown have documented that this lifetime component is an artifact and most frequently occurs with complex decays when utilizing the frequency domain MHF technology and the MEM data analysis software.[79,80] Data analysis indicates the presence of two real lifetime components, which can be attributed to phenol blue.

Surface and Branching Group Mimics. Mimics for PPI's surface (propylamine) and branching points (triethylamine) were also examined. Although these compounds do mimic parts of the dendrimer and provide information about the nature of chemical association, they do not mimic the effect of the dendrimer's three-dimensional structure. In general, the absorption spectra of phenol blue in these solvents have limited similarity to spectra obtained for the dye in dendrimer solutions. In relatively nonpolar triethylamine, phenol blue has a similar absorption λ_{max} (553 nm), as compared to its absorption in the dendrimers (λ_{max} 550 nm), but it does not fluoresce. Phenol blue also does not fluoresce in propylamine and absorbs outside of its solvatochromic range, which most likely indicates the formation of a ground-state complex.

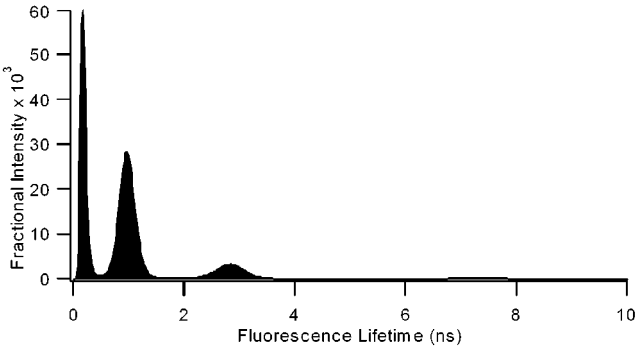

Figure 5. Representative MEM plot of the fluorescence lifetime distribution recovered for phenol blue [1×10^{-6} M] in G4 PPI [1×10^{-4} M]. Experimental conditions: $\lambda_{ex} = 514$ nm, $\lambda_{em} = 550-600$ nm, kaolin lifetime reference $\tau = 0$ ns, and $T = 25$ °C.

Calculation of Binding Constants. Phenol blue−dendrimer binding constants (K_D) were calculated assuming that the unassociated dye is predominantly monomeric, and these constants are shown in Table 1. The molar absorptivities at 654 and 554 nm were calculated for the free and associated dye from Beer's Law plots of the varying dye concentrations in water and in G4 PPI, respectively. However, even in G4 PPI, some small remaining amount of free dye still existed in solution. Therefore, the molar absorptivity of the associated dye was determined after deconvolution using the PeakFit program as described above. The following molar absorptivities were recovered: $\epsilon_{free:654} = 17\,500$, $\epsilon_{free:554} = 7700$, $\epsilon_{complex:654} = 1650$, and $\epsilon_{complex:554} = 8500$. It was assumed that the molar absorptivity of the dye−dendrimer complex does not change with dendrimer generation. The concentrations of associated and free dye were then calculated using Beer's Law for a system of two absorbing species with overlapping bands.

DISCUSSION

To fully understand and correctly interpret the experimental results, it is important to understand the implications of the dendrimer:dye ratio, which is 100:1. Using Poisson statistics, the probability, p_i, of finding i dye molecules in a single dendrimer is

$$p_i = \frac{n^i e^{-n}}{i!}$$

where n is the average number of dye molecules per dendrimer.

The probabilities that a single dendrimer contains zero, one, or more than one dye molecule are 0.990 05, 0.009 90 and 0.000 05, respectively. On the basis of these probabilities, the ratio of dendrimers containing a single dye molecule to those containing multiple dye molecules is 198:1. Therefore, the main source of the *associated* dye's fluorescence can only be attributed to the monomer form of the dye; all other forms (aggregate, excimer, exciplex, etc.) have negligible contribution.

The aforementioned monomer:aggregate probability ratio applies only to dye associated with the dendrimer. It does not apply to the unassociated phenol blue, solvated by water, nor does it mean that the dendrimers have sequestered the majority of the available dye. Aggregation of the unassociated dye is considerably more likely because of the dye's relatively low solubility. The equilibrium between associated and unassociated dye should favor dendrimer association as a result of the hydrophobicity of phenol blue and the relatively nonpolar interior of PPI. The exception would be in the presence of the smallest generations of PPI dendrimers, whose solvating abilities are more limited. This notion is supported by the absorption and fluorescence emission spectra, which demonstrate that the smallest-generation dendrimer has notably less sequestering ability.

Experimental results indicate that the dye definitely associates with the PPI dendrimers, and there are clearly two distinct dye populations. The nature of this dye−dendrimer association is characterized, in part, by studying the dendrimers' surface and branching group mimics. Although phenol blue has been shown to fluoresce in the presence of PPI dendrimers, no fluorescence is observed for either of the PPI dendrimer mimics, propylamine and triethylamine. Phenol blue's lack of observable steady-state fluorescence in these solvents and in water strongly suggests that phenol blue must be associated within the branches of the PPI dendrimers. The absence of any consistently apparent ground-state complex in absorption data, as seen to occur between phenol blue and the surface group mimic propylamine, also indicates that phenol blue is associated in the PPI interior region, beyond where the dye has any interaction with the dendrimer's surface.

The absorption and fluorescence λ_{max} values of phenol blue sequestered within PPI are indicative of a nonpolar microenvironment. All experimental results strongly suggest that the dye population within the PPI dendrimer interior is the origin of the absorption band at 550 nm and the predominant source of fluorescence emission. Furthermore, if the majority of the fluorescence emission signal originates from dendrimer-associated dye, it is also expected that this dye population will be responsible for the largest fractional intensity recovered in the lifetime distribution ($\tau_2 \approx 1.0$ ns).

The other absorption band at 654 nm is indicative of a much more polar, predominantly aqueous microenvironment and is considerably less intense in all generations but G1. As such, very little fluorescence emission is expected from this aqueous dye population. This expectation is confirmed by the trend of increasing relative fluorescence intensity with increasingly larger generations. These facts further support the assignment of the second lifetime component, τ_2, as the dendrimer-associated dye population. Although phenol blue is only weakly fluorescent in water, under lifetime measurement conditions, which employ a broad emission window via filters, one real lifetime component (τ_3) is reproducibly recovered for this sample. This component is most likely due to an aggregate of the relatively hydrophobic dye molecules in water. The heterogeneity in the third lifetime component ($\tau_3 = 2.99 \pm 0.33$) supports this assumption, because the exact composition of the dye aggregate will vary. The MEM plot in Figure 5 clearly shows that this lifetime component (τ_3) is not discrete, but rather, is distributed. Examination of the lifetime distributions for phenol blue in aqueous dendrimer solutions clearly illustrates that the third lifetime component is due to the unassociated dye present in these solutions. The fact that τ_2 is less than τ_3 may seem surprising, but we have discovered that the lifetime of phenol blue is also sensitive to solvent polarity.[86] In neat organic solvents, its lifetime decreases with increasing solvent dielectric constant.[86]

Although absorption spectra and fluorescence lifetimes clearly show two dye populations in the presence of all of the PPI generations, it is not surprising that only one population is apparent in the steady-state fluorescence emission spectra. The dynamic lifetime measurement distinguishes between the two fluorescence signals even when only one is observed in steady-state measurements. In steady-state mode, one band may obscure another as a result of its width, close wavelength proximity, and significantly greater intensity. The use of 514 nm as the excitation wavelength may also be a contributing factor; however, the dye's very broad absorption band does encompass this wavelength region.

Fluorescence lifetimes also provide additional microenvironmental information. In general, they are known to lengthen as a fluorophore is sequestered into an increasingly rigid or more protected microenvironment, such as micelles, cyclodextrins, or dendrimers; however, in our data, there does not appear to be a trend toward longer lifetimes with increasing dendrimer generation for the lifetime of the dendrimer-associated dye, τ_2. This lifetime data suggests that phenol blue experiences a very similar microenvironment in terms of structural rigidity and accessibility for the generations studied. Examination of the dendrimer structure reveals that only the microcavities near the core would remain unchanged from one generation to the next. Therefore, this may be the specific location of phenol blue within the dendrimer interior.

Changes in the microenvironmental rigidity of the fluorophore are also generally observed as increases in steady-state anisotropy values, because a more rigid/protected microenvironment hinders rotational diffusion. Steady-state anisotropy is directly dependent on the rotational correlation time, is inversely related to the fluorescence lifetime,[75] and is a measure of the average rotational motion of the fluorophore. Microenvironmental rigidity can be the most prominent contribution to this decay; however, in this case it must be a minor contribution to the total signal, because the lifetimes (τ_2 and τ_3) and fractional intensity ratio of associated to unassociated dye (α_2:α_3) do not appear to change with generation, but the anisotropy values do increase in a systematic fashion. Therefore, the fairly linear trend in the anisotropy data is best explained by the molecular volume increase seen with dendrimer generation. The limiting anisotropy of the probe could not be measured for comparison because of its lack of fluorescence

(86) Richter-Egger, D. L.; Tucker, S. A. Unpublished results, 2001.

in solvents such as glycerol; however, it is expected to be close to the theoretical limit of 0.4.

Generational Dependencies. The absorption spectrum of phenol blue in G1 PPI is distinctly different from the aqueous phenol blue solution as well as the spectra of the other dendrimer generations. The absorption and fluorescence spectra from this solution show that the dendrimer does protect the dye from water. Although the deconvoluted absorption spectrum contains two bands (632 and 531 nm), neither is in the same location seen in the other generations for the free dye (654 nm) or the associated dye (554 nm). The 588-nm λ_{max} of the fluorescence band indicates a somewhat nonpolar microenvironment but one that is still more polar than that afforded by the larger-generation PPI dendrimers. Given that the anisotropy data shows a relatively "loose" association, as compared to other generations, only one or perhaps a couple dendrimers are most likely to be associated with a single dye molecule. It is clear that extensive dendrimer aggregation around phenol blue does not occur, because this would result in a microenvironment that is significantly more restrictive than what is observed in the anisotropy measurements.

The three largest generations (G3, G4 and G5) have statistically indistinguishable absorption and fluorescence λ_{max} values, indicating that all provide microenvironments of essentially equal microenvironmental polarity. The 550-nm absorption λ_{max} is very near to that observed for *n*-heptane. In the absorption data, the amount of unassociated dye (λ_{max} 654 nm) is observed to decrease slightly with increasing generation; however, the ratio of the lifetime fractional intensities, α_2:α_3, does not consistently increase or decrease with increasing generation, indicating that the these larger-generation dendrimers have nearly equal abilities to sequester the dye.

Overall, these results indicate that the dye−dendrimer association very nearly eliminates the interaction of the dye with water for the three largest generations and that these dendrimers are all able to sequester the vast majority of phenol blue, provide nearly equal nonpolar microenvironments, and are kinetically alike over a 48-h period.

Comparison to PAMAM-AT Dendrimers. The PAMAM and PPI dendrimers continue to be the only commercially available dendrimers. These two dendrimer families are similar in that both utilize the same branching point structure and are available in amine-terminated forms. Important differences between PAMAM and PPI are the length of their initiator cores (diaminoethane and diaminobutane, respectively), the length of their branching units (eight and four bonds, respectively), and the chemical nature of their branching units (alkyl chain with amido group vs alkyl chain, respectively). When visualized in a two-dimensional (2-D), extended conformation, the smaller-generation PPI dendrimers have a more open structure as a result of the larger initiator core; however, this relationship eventually reverses for progressively larger-generation dendrimers because of the PPI dendrimers' shorter branching unit. The measured diameters of the PAMAM and PPI dendrimers in dilute aqueous solutions are reported to be ∼10 and 5 Å/generation, respectively.[6,47,87,88] The effects of these structural differences have very interesting implications on the comparative chemical and physical properties of these two dendrimer families.

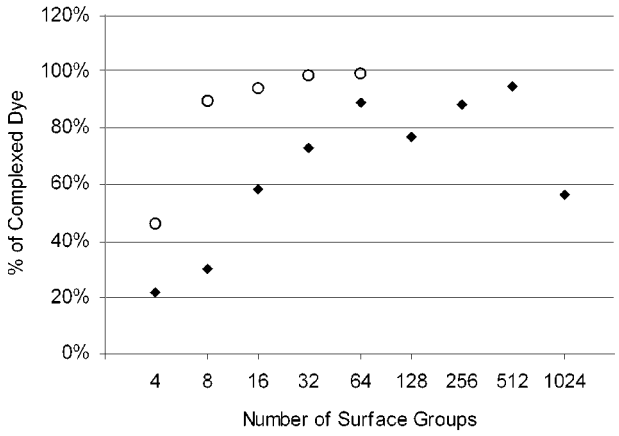

Figure 6. Plot of representative data for the percentage of complexed dye for phenol blue [1×10^{-6} M] in the PPI (○) and PAMAM (◆) dendrimers [1×10^{-4} M]. The percent of complexed dye was determined on the basis of the *calculated* amounts of free and complexed dye.

Clearly, to most accurately describe the effects of these stated differences, it would be best to compare or change them one at a time. However, because these two commercial dendrimer families are examined under exactly the same experimental conditions, it is still beneficial to compare and contrast them here to ascertain some of their similarities and differences as solvated species and to illustrate the value and advantages of spectroscopic probe measurements.

Before we can begin such a comparison, their generational nomenclature must be addressed. Unfortunately, dendrimers from each family having the same number of surface groups do not share the same generation number. Generation 1 PAMAM has eight surface groups while G1 PPI has four surface groups, the same as G0 PAMAM. Because they both have the same branching pattern, which results in the number of surface groups as powers of two (i.e., 4, 8, 16, 32, ...), we will make comparisons by the number of surface groups (SG) rather than by generation number.

In general, the absorption and fluorescence emission data indicate that the PPI dendrimers, with an equivalent number of SG, provide slightly less polar microenvironments (Table 1). (This trend is clearer in the averaged data from many experiments, not presented here.) This is expected and is easily explained by the presence of the more polar amido group in the PAMAM dendrimers. Although visual inspection of both sets of absorption spectra could lead to similar findings, a more quantitative analysis also provides additional information about the percent of dye that is complexed by the dendrimer (Figure 6), as well as the binding constants (Table 1). (The previously unreported phenol blue−PAMAM-AT binding constants were obtained in a similar fashion as those determined for PPI; see Table 1 footnote for additional details.) Not only do the PPI dendrimers complex more of the dye than PAMAM dendrimers with the same number of SG, but each of the four largest PPI dendrimers that were studied complexes ∼100% of the dye (Figure 6). The dye−dendrimer binding constants (Table 1) have similar comparative implications, generally an order of magnitude larger for the PPI versus PAMAM dendrimers of an equivalent number of SG.

(87) Topp, A.; Bauer, B. J.; Tomalia, D. A.; Amis, E. J. *Macromolecules* **1999**, *32*, 7232−7237.
(88) Topp, A.; Bauer, B. J.; Prosa, T. J.; Scherrenberg, R.; Amis, E. J. *Macromolecules* **1999**, *32*, 8923−8931.

While the PPI dendrimers begin complexing the vast majority of the dye as early as eight SG (G2 PPI), the data indicate that the binding constants of progressively larger-generation PAMAM dendrimers increase in a much more incremental, almost linear fashion through 64 SG (G4 PAMAM). The deviation from this trend by 128 SG (G5 PAMAM) is a good example of the effects of the shape change (from "dumbbell-like" to more spheroidal) that reportedly occurs between these two generations of PAMAM dendrimers.[37,89] Another important observation is that the binding constant for 1024 SG (G8 PAMAM) decreases almost an order of magnitude from the previous generation and is best explained on the basis that the surface of the dendrimer has become sufficiently crowded[90] as to hinder the movement of the dye in and out of the dendrimer. As stated in our previous paper,[39] we believe that dye−dendrimer association is kinetically slower for G8 PAMAM. These observations and explanations also apply to the percent of dye complexed by G5 and G8 PAMAM. Further examination of the absorption and fluorescence data indicate that the larger PPI core provides a better "fit" for the phenol blue molecule, which is also supported by the steady-state anisotropy data.

Generally, the fluorescence anisotropy values increase systematically for both dendrimer families. However, proceeding from the smallest to the largest dendrimer generations, anisotropy values for the PPI dendrimers start smaller and increase at a faster rate than do the values for the PAMAM dendrimers (Table 1). The difference in the anisotropy trends for PAMAM and PPI accurately reflects their structural differences, as portrayed in the 2-D structure, where PPI begins as more open structure (4 SG). One would also expect that its density would increase at a faster rate for progressively larger generations. Significant macromolecular shape changes (from one generation to the next) are also visible in the anisotropy values for both dendrimers occurring between four and eight SG for PPI (G1−G2) and 64−128 for PAMAM (G4−G5). Other reports have also noted this shape change for the PAMAM dendrimers.[27−30,89,91−94] The anisotropy values for the PAMAM dendrimers are also observed to remain relatively constant for the three largest generations. No similar occurrence exists for those PPI generations studied, although inclusion of larger-generation PPI dendrimers, which are not currently available, in this type of study may very well demonstrate similar behavior.

Fluorescence lifetime data indicates similar microenvironmental rigidity for both PAMAM and PPI dendrimers, because neither τ_2 nor τ_3 is statistically different between these two families. Otherwise, the lifetime data confirms observation already made on the basis of absorption and fluorescence emission spectra. The ratios of α_2:α_3 reinforce the observations that the amount of complexed dye gradually increases with increasing generation for PAMAM and that almost all of the dye is complexed in some form for all of the generations of PPI dendrimers studied.

There are a few generational inconsistencies in these studies. The anomalies created by a kinetic effect for G8 PAMAM have already been discussed in detail; however, the fluorescence emission of phenol blue in G5 PPI still needs to be addressed. The G5 PPI steady-state fluorescence intensity is significantly decreased, approximately the same as G1 PPI. This decrease in fluorescence is not due to less dendrimer-associated dye, as seen for G8 PAMAM, or formation of a ground-state complex, because no significant difference is observed in the absorption spectra between G4 and G5 PPI. No changes in microenvironmental polarity or rigidity are observed in the fluorescence data, either; therefore, dynamic-state quenching must occur that does not result in an additional fluorescence signal. We believe that this quenching is due to the dendrimer's tertiary amine groups, because they have been observed to quench the fluorescence of pyrene.[25,37,54] This is the only dendrimer generation (PPI or PAMAM) in which we observed fluorescence quenching of phenol blue. It is important to note that the extent of quenching observed for phenol blue is considerably less than what has been observed for pyrene in PPI or PAMAM dendrimers.[25,37,54] It appears that a better "fit" between phenol blue and PPI dendrimers may make the G5 PPI dendrimer, which has the greatest number of tertiary amine groups, more likely to quench phenol blue fluorescence as these groups are forced into closer proximity to the associated dye molecules.

In addition, information about the size of the dendrimer cavities can be ascertained from other studies in the literature. Nile red (phenoxazon-9), a previously mentioned structural analogue of phenol blue that is only somewhat larger, did not associate with the PAMAM dendrimers' interior cavities.[73] Therefore, it can be speculated that the cavity size is between the molecular volume of Nile red and phenol blue. It should also be noted that Nile red was encapsulated in PAMAM dendrimers with extended cores (C12 vs C2).[73] Studies of the PPI dendrimers with Nile red are ongoing.

CONCLUSIONS

The physical properties of the interior regions of PPI dendrimers were studied through the association of the spectroscopic probe phenol blue. These data clearly showed the existence of two different dye populations in the presence of each generation studied, although the unassociated dye population was extremely small in the larger-generation PPI dendrimers. In general, PPI dendrimers bind nearly all of the available dye into a tight, nonpolar microenvironment. The polarity within the PPI dendrimer microcavities was shown to be similar to that of *n*-heptane and is in agreement with the previous study[54] of G4 and G5 PPI using pyrene. Studies of the surface group mimics clearly showed that the majority of the dye did not associate at the dendrimers' surface, but rather within the dendrimers' microcavities, where phenol blue was completely encapsulated, near the core. The second dye population consisted of a small remaining portion of the dye in the form of an unassociated self-aggregate and was the result of the dendrimers' inability to truly sequester 100% of phenol blue in solution.

This research effectively draws distinction between G1 and G3−G5 PPI by demonstrating that the all of larger dendrimers

(89) Naylor, A. M.; Goddard, W. A., III; Kiefer, G. E.; Tomalia, D. A. *J. Am. Chem. Soc.* **1989**, *111*, 2339−2341.
(90) de Gennes, P. G.; Hervet, H. *J. Phys. Lett.* **1983**, *44*, 351−360.
(91) Meltzer, A. D.; Tirrell, D. A.; Jones, A. A.; Inglefield, P. T.; Hedstrand, D. M.; Tomalia, D. A. *Macromolecules* **1992**, *25*, 4541−4548.
(92) Meltzer, A. D.; Tirrell, D. A.; Jones, A. A.; Inglefield, P. T.; Hedstrand, D. M.; Tomalia, D. A. *Macromolecules* **1992**, *25*, 4549−4552.
(93) Gao, Y.; Langley, K. I.; Karasz, F. E. *Macromolecules* **1992**, *25*, 4902−4904.
(94) Prosa, T. J.; Bauer, B. J.; Amis, E. J.; Tomalia, D. A.; Scherrenberg, R. *J. Polym. Sci. B* **1997**, *35*, 2913−2924.

have similar and comparatively large binding affinities for the dye molecule. The effective microenvironmental polarity was observed to decrease with increasing generation up to G3, after which it remained constant. Experimental data for G2 PPI indicated a transition between the two different microenvironments afforded by the G1 versus G3−G5 PPI dendrimers.

The previously unanswered, fundamental questions regarding the flexibility and rotational freedom inside the dendrimers microcavities have also been addressed here. Systematic increases in anisotropy values were descriptive of increases in molecular volume with increasingly larger generations of PPI dendrimers. Fluorescence lifetime information indicated that the rigidity of the microcavity where phenol blue was sequestered within the dendrimers was not dependent on generation, although this cannot be confirmed by steady-state fluorescence anisotropy measurements because of large contributions to the anisotropy from the dendrimers' increasing molecular volume with generation. The rotational freedom specific to the phenol blue molecule in the microcavity cannot be distinguished from the rotational motion of the dye−dendrimer complex until improved methods of modeling dynamic anisotropy for complex, multiexponential decays are developed.

The comparison of amine-terminated PPI and PAMAM dendrimers clearly demonstrated the effects of their structural differences and the ability of phenol blue to sense those differences: (1) the effects of the chemical functionality (alkyl chain vs alkyl chain with amido unit), resulting in a slightly less polar microenvironment within the PPI dendrimers; and (2) the effect of the initiator core length (diaminobutane and diaminoethane) and branching unit length (four bonds vs eight bonds), resulted in a more rapid transition with increasing generation to higher PPI binding constants and initially lower, but more rapidly increasing PPI anisotropy values. Shape transitions were also demonstrated in the binding constants and anisotropy data for both dendrimer families.

ACKNOWLEDGMENT

The authors thank Jeff C. Landry and Spencer J. Flamm for their assistance with some related experiments. This research was supported in part by the University of Missouri−Columbia, Life Sciences Undergraduate Research Opportunity Program (LSUROP) awarded to A. Tesfai and grants from the National Science Foundation (CAREER Award Grant no. CHE-9733853) and the University of Missouri−Columbia, Research Council.

Received for review June 20, 2001. Accepted September 25, 2001.

AC0155355